GLL

Geomatics, Landmanagement and Landscape No. 1 • 2024, 117–133

ISSN 2300-1496 http://dx.doi.org/10.15576/GLL/2024.1.08

Research paper

Received: 07.01.2024
Accepted: 04.02.2024
Published: 15.06.2024

Exploring the economic significance and diverse hues of quartz: A case study at Adaila, south of El Ma Labiod, NE Algeria

Wassila Nacer[1,✉] 0009-0003-3879-9735
Nabil Defaflia[1] 0000-0002-6943-3416
Hassan Taib[2] 0000-0001-7990-2258
Rofaida Rehebi[1] 0009-0004-7110-1631

[1] Department of Earth and Universe Sciences, Larbi Tebessi University, Tebessa, Algeria, Laborarory of Sedimentary Environment, Mineral and Hydric Resources of Algeria Eastern, Faculty of Exact Sciences, Sciences of Nature and Life, University Echahid cheikh Larbi Tebessi, Algeria

[2] Department of Geology, Laboratory of Natural Resources and Management of Sensitive Environments (LRNAMS), Faculty of Earth Sciences and Architecture, Larbi Ben M'hidi University, Oum El Bouaghi, Algeria

✉ Corresponding author: wassila.nacer@univ-tebessa.dz

Summary

The Tebessa region in Algeria is rich in mineralogical resources within its Quaternary deposits, particularly in quartz. This study adopts a multidisciplinary approach including stratigraphic, sedimentological, and granulometric analyses, focusing specifically on the deposits located in the fluvial terraces of the Oued Adaila, south of Tébessa in eastern Algeria. The analysis of granulometric parameters gave valuable insights into the uniformity of the energy levels exerted by the transport agents.

Pioneering exoscopy techniques have proved indispensable in discerning the sedimentary history of quartz, offering comprehensive insights into its weathering processes and its intricate journey through continental aquatic pathways. Additionally, this methodology has elucidated the genesis of unique colourations observed in quartz grains. Using Scanning Electron Microscopy (SEM), we have examined the surfaces of quartz grains, revealing an array of patterns attributable either to the inherent crystal lattice structure of quartz or to the erosive influences of the changing environment. These environmental modifications stand out as the primary contributors to the diverse spectrum of colours manifested in the quartz grains.

Furthermore, the examination of magnetic data has highlighted the pivotal role played by various oxides present in the Quaternary deposits. These oxides proved to be important sources of ferric elements, crucial in imparting the distinct colorations observed in quartz. This comprehensive study significantly advances our understanding of the mineralogical constitution, sedimentary evolution, and the environmental dynamics shaping the Quaternary deposits in the Tebessa region.

Keywords

ferric elements • granulometric parameters • Quaternary • Oued Adaila • quartz colouring

1. Introduction

The quartz (SiO_2) is one of the most common minerals in the Earth's crust, found in various geological settings. Distinct appearances of quartz depend on different formation circumstances It also exhibits a remarkable resistance to both chemical and physical forces [Wicander an Monroe 2005]. Quartz occurs mainly as sand residue from rock weathering, covering large areas of the Earth's surface. While most abundant in granites and similar rocks, quartz almost exclusively constitutes quartzite and sandstone, along with calcite.

Characterised by its widespread distribution and exceptional resistance to weathering, quartz occupies a important place among the constituents of soils and a substantial portion of the Earth's crust. Constituting about 12% of the crust, quartz is the second most abundant mineral on Earth, after feldspars, which make up over 60% of its total [White 2006, Schaetzl and Anderson 2015]. Due to its SiO_2 composition, quartz possesses a vitreous luster, making it one of the finest minerals. However, apart from its silica base, quartz can also contain various additional elements/compounds (Al, Ti, Fe, Na, K, Mg, Ca, OH) as interstitials or isomorphous substituents, including coatings such as Fe and Mn oxide minerals [Dennen 1966, Dahoua et al. 2020]. These components, together with the climatic conditions during quartz formation, contribute to variations in its properties, including colour.

In recent times, mineral resources have attracted substantial attention across global industries, and quartz is no exception in Algeria or worldwide. Whether in macrocrystalline form in jewellery and watchmaking or in microcrystalline form in glassmaking, quartz holds economic significance due to its optical properties and the impurities encapsulated in its grains.

The study area, situated in the El Ma Abiod region within the Saharan Atlas of eastern Algeria, is characterized by Maastrichtian limestone formations oriented NE-SW, interspersed with a moi-quaternary depression (El Ma Abiod plain). The complex geological features, including the defined anticlines, synclines, and fault systems, heavily influence the region's landscape and geological orientation [Laffite 1939, Zerzour et al. 2020]. Our study attempts to comprehensively investigate the granulometry, morphoscopy, and colouration of the Quaternary formations within the Oud Adaila alluvial terraces. Employing a stratigraphic, sedimentological, and granulometric approach, the research aims to uncover the various aspects of these formations.

The prominence of quartz within this particular area is remarkable. Its varied colour spectrum, ranging from transparent white to hematoid red, makes the mineral stand out amidst the geological tapestry. Through a multidisciplinary lens including stratigraphic, sedimentological, and granulometric perspectives, the study seeks to achieve the following objectives:

- Construction of a stratigraphic log,
- Definition of granulometry, morphoscopy, and magnetism within the study area,
- Identification of different colours present in the study site,
- Determination of causes contributing to quartz coloration,
- Estimation of the percentage prevalence of the most dominant colour.

This holistic investigation aims to provide comprehensive insights into the multifaceted nature of quartz minerals, shedding light on their stratigraphic, sedimentological, and colouration attributes within the specified region.

2. Study area

The Adaila site lies to the south of the El Ma Labiod plain, positioned southwest of the wilaya of Tébessa and roughly 250 km from the Mediterranean Sea (Fig. 1A). Its northern border is marked by a diverse mountainous landscape, characterized by the Jebels Doukkane, Anoual, and Bouroumane.

The geological layout of the El Ma Abiod plain has evolved through distinct tectonic phases, notably the Atlasic phase spanning between the Upper Lutetian and Lower Miocene periods, succeeded by the Miocene phase [Zeqiri et al. 2019, Kerbati et al. 2020]. Within this area, three significant fault systems intersect, oriented along NE-SW, NW-SE, and E-W directions, meticulously documented by Tamani et al. [2019], Boulemia et al. [2021], Mahleb et al. [2022], Chibani et al. [2022], and Taib et al. [2022, 2023a, 2023b, 2024].

Although the El Ma El Abiod plain has not been geologically examined, it belongs to a larger geological complex that has received relatively more attention. Exploratory drilling and geophysical surveys have been conducted since the 1970s, primarily focused on water and oil.

The climate of this region is determined by an average altitude of 1354 m, and so it is a semi-arid with temperatures ranging from 6.88°C to 25.05°C and an average rainfall of 204 mm/year. The region is more prone to drought due to a highly irregular rainfall pattern, mainly dry seasons with low rainfall [Benmarce et al. 2021].

The sedimentary formations within the El Ma El Abiod sub-watershed consist of several distinct layers:

- Epicontinental type deposits exhibit variations in facies and thickness, predominantly oriented in NE-SW direction, spanning from the Aptian to the Maestrichtian periods.
- Presence of Miocene-based sandstones and variegated clays.
- Germanic Triassic formations, often in diapiric form.
- Miocene bariolate sandstones and clays.
- Germanic Triassic formations, are frequently observed in diapiric configurations.

The NW-SE geological cross-section (Fig. 1B) extends from the J. Guelia syncline to the Anoual anticline of the study area. Several geological features characterize the El Malabiod study region.

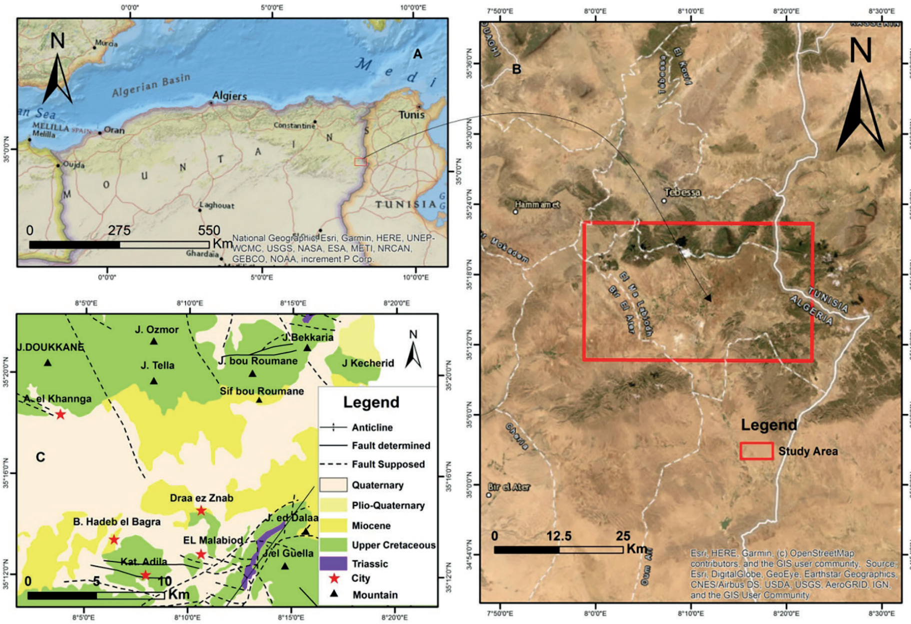

Source: Authors' own studies

Fig. 1A. Location map of the study area

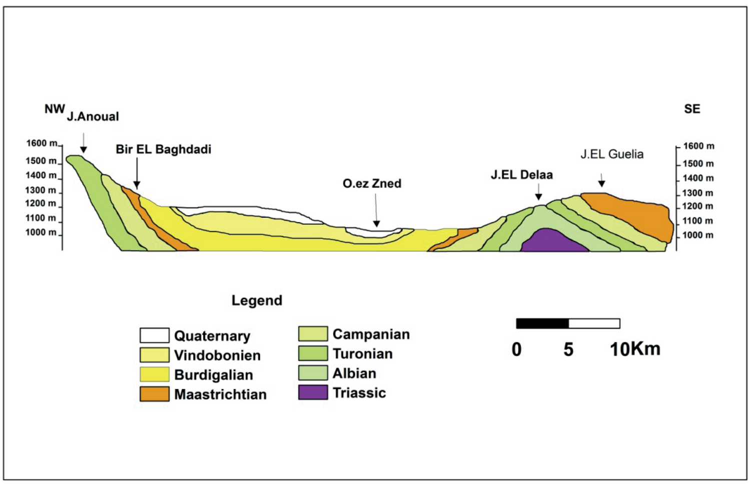

Source: Authors' own studies

Fig. 1B. Geological cross-section of the study area

3. Material and methods

This research involved analyses were carried out in the laboratory.

3.1. Sedimentological analysis

Granulometric analyses: Performed using a Mastersizer 2000 granulometer employing laser diffraction. Both crude and decalcified fractions of samples sieved to 2 mm were analysed. Parameters were calculated using the granulometer manual [Mastersizer 2000] and interpreted based on works by Folk and Ward [1957], Rivière [1977], Pye and Blott [2004], Anderson [2007], and Miskovsky [2002].

Morphoscopic and exoscopic studies of quartz grains: Selected quartz grains were subjected to binocular loupe selection and examined using a Philips XL 30 Environmental Scanning Electron Microscope equipped with an EDAX microprobe. The identification method followed the recommendations of Ribault [1977].

Magnetic methods: Employed to reveal deposition variations, classify materials, identify transport and formation processes of magnetic grains, and propose paleoclimatic interpretations. All measurements were conducted on unoriented, dried samples consolidated with an aqueous sodium silicate solution

3.2. Stratigraphic analysis

Description of geological layers, emphasizing average thickness, texture, colour, boundary characteristics, visible macro-structures, and specific features such as hydromorphy, stains, roots, or prehistoric artifacts.

Emphasis on differentiating between the geological layer itself and any subsequent pedological alterations.

3.3. Granulometric analysis

Technique for segregating particles into granulometric fractions based on size statistics.

Aims to identify substances associated with these fractions in sediments and to reconstruct particle transport and deposition conditions. Classification based on Table 1.

Granulometric analysis allows the reconstruction of sediment substances found in fine, medium, or coarse fractions, in which helps to understand particle transport and deposition conditions within the study area.

Table 1. Granulometric distribution of sediment constituents

Element diameter	Granulometric class	Granulometric fraction
Above 10 cm	Blocks	Coarse fraction
From 01 cm to 10 cm	Stones or pebbles	
From 1 cm to 2 mm	Granules, gravel	

<table>
<tr><th>Element diameter</th><th>Granulometric class</th><th>Granulometric fraction</th></tr>
<tr><td>From 0.2 mm to 2 mm</td><td>Coarse sands</td><td rowspan="4">Fine fraction</td></tr>
<tr><td>From 40 µm to 0.2 mm</td><td>Fine sands</td></tr>
<tr><td>From 2 µm to 40 µm</td><td>Limons or powders</td></tr>
<tr><td>Below 2 µm</td><td>Clay</td></tr>
</table>

Source: adapted from Miskovsky and Debard [2002]

3.4. Morphoscopy of quartz grains

This study, developed by Cailleux and Tricart [1959], is applied to quartz grains in the fine fraction. It is carried out using a binocular magnifying glass, and it is supposed to examine the shape and appearance of quartz grains under the following observation conditions.

The grains, washed with water or hydrochloric acid (cold or hot), are dried and then observed with a binocular loupe, isolated dry and against a black background. This provides information on how these grains are transported. Several types of quartz grains can be distinguished.

3.4.1. Transparent Non-strained

Quartz with angular contours and limpid appearance. Their faces are flat and smooth, with breaks.

3.4.2. Opaque Non-strained

Quartz of the same shape as above, but with a dull appearance. These two types of grain have either not been transported, or have been transported but have not had time to leave their mark (scree, torrents, etc.).

3.4.3. Transparent transparent flat transparent flat

Quartz with transparent flat, rounded corners. They are limpid.

3.4.4. Opaque transparent flat transparent flat

Quartz of the same shape as above, but with a transparent flat appearance. Shiny or opaque transparent flat quartz grains characterize long-lasting transport by water. Perfectly ovoid grains have been formed in karstic environments.

3.4.5. Round

Circular-shaped quartz with traces of shocks that indicate that it is transported by the wind. In addition to these different forms of quartz grains.

Other intermediate forms were found in our study area, such as the sub-transparent flat.

4. Exoscopy of quartz grains

Quartz exoscopy studies the different types of traces of chemical, physical or mechanical origin that have modified the original appearance of the external surface of quartz grains [Le Ribault 1977]. The method makes it possible to differentiate the traits acquired by the quartz grain in its current sedimentation medium from the traits retained from one or more previous media.

The quartz grains were selected for exoscopic study with a binocular magnifying glass. The observations were made with the Philips XL 30 environmental scanning electron microscope equipped with an EDAX microprobe.

4.1. Apparatus (scanning electron microscope)

Scanning electron microscopy works by emitting electrons from a cathode and detecting signals from the interaction of these electrons with the sample. These electrons, which irradiate the surface of the sample, penetrate deep into the material and affect a volume called the 'interaction bulb' (Fig. 2).

This volume depends on the average atomic number of the sample and the energy of the incident electrons. In this interaction volume, the electrons in the beam lose their energy through multiple collisions with the atoms of the material, generating numerous secondary phenomena: re-emission of electrons and photons, absorption of electrons, induced currents, electrical potentials, local temperature rise, lattice vibrations.

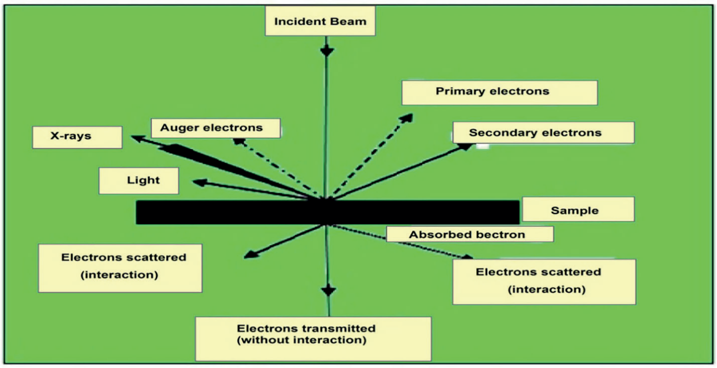

Source: Authors' own studies

Fig. 2. All the radiation that can be emitted during interaction between an electron beam and a sample

4.2. Magnetic analysis

Magnetic methods make it possible to: 1) reveal the variations, particularly in the depositional mode, which are not necessarily visible to the naked eye, 2) classify different types of material, 3) identify the transport and formation processes of magnetic grains, 4) propose a paleoclimatic interpretation [Djerrab and Aïfa 2010a, Djerrab and Hedley 2010b].

All magnetic measurements were carried out on unoriented samples, dried and consolidated with an aqueous sodium silicate solution to prevent grain movement during handling. The following magnetic properties were measured.

5. Results and discussion

Macroscopic observation in the field allowed us to subdivide the 380 cm thick geological section into twelve different stratigraphic levels, indexed from A to L (Fig. 3).

Level A: (0 to –30 cm) granular in texture and blackish (dark) in colour, consisting mainly of gravel (55%) and pebbles (15%). The rate of weathering is low. Carbonate content varies between 23 and 33%. This level contains a few plants and organisms. Porosity is high, hardness low. Flints present.

Level B: (–30 to –50 cm) beige gravel and pebbles. Porosity is low and hardness high, with a carbonate content between 21%.

Level C: (–50 to –80 cm) beige granular texture, alternating fine matrix and pebbles. The rate of weathering is low. Carbonate content varies between 31 and 32%. This level contains roots.

Level D: (–80 to –120 cm) alternating fine matrix, gravel and pebbles. This level is very rich in small gravels, indurated by calcareous water, and beige in colour. The fine elements are mainly silt and fine sand. The percentage of carbonates varies between 24 and 37%. Low porosity and high hardness, with the presence of flints and roots.

Level E: (–120 to –160 cm) beige granular texture, fine matrix with small gravels. Carbonate content varies between 25 and 38%. This level contains a few roots, and average porosity is hard.

Level F: (–160 to –180 cm) beige, granular texture, composed mainly of gravel (55%) and pebbles (15%). Carbonate content varies between 19 and 41%. This level contains roots. Porosity is low, hardness is high, and the level is rich in flint tools.

Level G: (–180 to –220 cm) fine granular matrix, beige in colour. Carbonate content varies between 26 and 34%. This level contains roots. Porosity is low, hardness is high, and the level is rich in flint tools.

Level H: (–220 to –250 cm) alternating fine matrix with gravels of granular texture and beige colour. Carbonate content varies between 22 and 59%, with low porosity and high hardness.

Level I: (–250 to –280 cm) granular texture and beige colour, mainly gravel (65%) and pebbles (35%). Carbonate content varies from 27 to 53%, with high porosity and low hardness.

Level J: (–280 to –320 cm) beige granular texture, composed mainly of gravel (45%) and pebbles (35%). Carbonate content varies between 20 and 56%. Average porosity and hardness.

Level K: (–320 to –350 cm) alternating fine matrix and gravels with the presence of beige boulders. Carbonate content varies between 30 and 45%. Porosity is hardness is high.

Level L: (–350 to –380 cm) fine matrix with granular-textured, beige-coloured boulders. Carbonate content varies between 29 and 35%. Porosity is medium, hardness high.

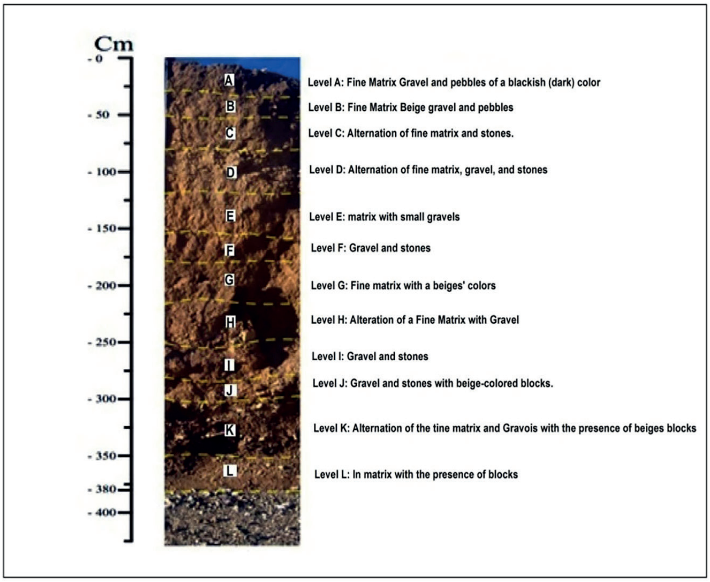

Source: Authors' own studies

Fig. 3. Stratigraphic log of the study area

The sedimentological study included 50 samples taken systematically from the top to the bottom of the stratigraphic section.

A study of the overall granulometric composition (Fig. 5) identified twelve stratigraphic levels, some rich in coarse fraction (gravel and pebbles) alternating with silt-rich levels. The percentage of clay fraction is very low and remains more or less constant throughout the stratigraphic section.

A study of the overall particle size composition (Fig. 5) reveals several stratigraphic levels, some rich in coarse fraction (gravel and pebbles) alternating with silt-rich levels. The percentage of clay fraction is very low and remains more or less constant throughout the stratigraphic section.

The granulometry of the fine fraction (Fig. 5) shows a relatively uniform sediment, with very little clay (1.4% on average), a high silt content (60%), and moderate percentages of fine and coarse sands (15% and 17%, respectively). The evolution of the latter is similar to that of gravel and pebbles. The exception is level B, where the silty fraction increases at the expense of the coarse fraction (coarse sand). In level L (at the base), the proportion of fine sands increases at the expense of coarse sands.

According to the ternary diagram (Fig. 4), the sediments are essentially composed of sand silts . Deposits in the lower part are located in the specific silt zone.

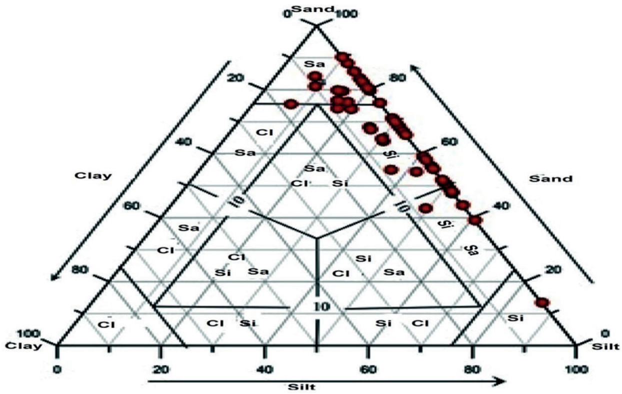

Source: Authors' own studies

Fig. 4 Diagram of the various fractions of the overall granulometry of section 3 (gravel, pebbles, sand, silt, clay)

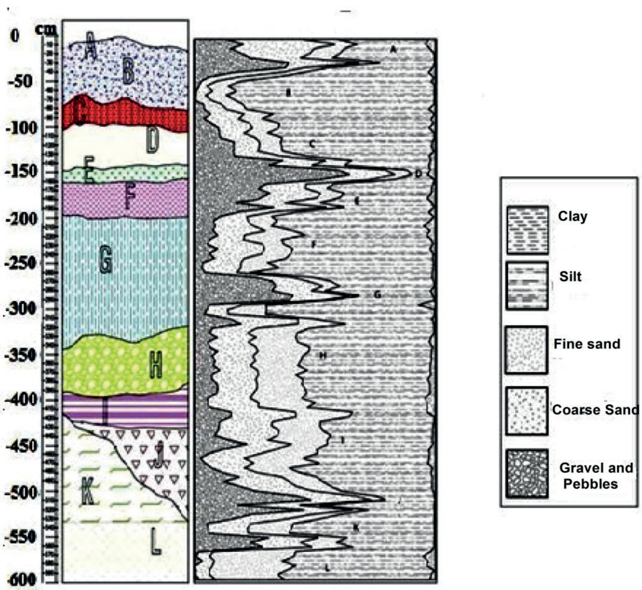

Source: Authors' own studies

Fig. 5. Grain size fractions in the ternary diagram of section 3.The morphology of quartz grains

Quartz grains were examined using a binocular magnifying glass on the grain fraction between 0.315 and 0.500 mm. This fraction best records the physical actions of the environment [Le Ribault 1977].

The study revealed a high percentage of transparent flat or strained grains (U) (Fig. 6). Their appearance indicates that these grains have undergone significant reworking before their final deposition. We also note the presence of a small percentage of matte round grains (RM), originating from Miocene sandstone, which occupies large parts of the region.

We also note the presence of angular to sub-angular non-strained grains (indicating short transport close to the parent rock). Rounded grains also occur, but in very small quantities. Quartz grains are in the minority compared to calcite grains (over 80% of the elements attacked by HCL).

In fact, the richness of transparent flat grains and the dominance of angular sub-grains allow us to come to conclusion that they were transported by water, and thus to propose a predominance of the Aeolian factor. However, we feel that this hypothesis needs to be confirmed by an exoscopic study of these grains in order to specify the mode of transport and also to check whether the grains show characteristic traces of impact or friction.

All the grains observed proved to be pedogenetic quartz with very pronounced physico-chemical alteration features.

Exoscopy allowed us to differentiate the sedimentary history of the quartz (alteration, transport by land or water).

Source: Authors' own studies

Fig. 6. Morphoscopy of Level 5 quartz grains

The quartz grains in this section show several traces of mechanical origin. These traces are often exploited by chemical alteration phenomena, reflecting a final stage in the pedogenetic evolution of this quartz (Fig. 7). The shape of many quartz grains indicate previous eolianization phases, such as crescents and V-shaped impact marks that point to fluvial mobilization. This mobilization is enabled by the waters of the wadi. Other shapes, such as conchoidal fractures with polishing gradients, indicate an aquatic evolution.

Chemical changes in this environment depend on emersion and immersion phenomena, which alternate periodically: during emersion, water trapped in depressions becomes highly concentrated in silica due to evaporation, favouring siliceous precipitation of various forms.

This study was carried out using a binocular and was focused on the condition and colour of quartz grains . The characteristics visible on the surface of these grains were caused by physical and chemical factors, which are reflected in the differences in quartz colouration. Most grains have a glassy-white to translucent-white colour, occurring in 75% of grains. The second most important colour is translucent yellow and orange to orange-red (10% and 15%), while some grains are half vitreous white and half orange. The last colour present in the samples – its percentage is insignificant – is translucent violet. Despite its very rare occurrence, this colour is interesting because the vitreous yellow colour of quartz comes from this colour (percentage 5%).

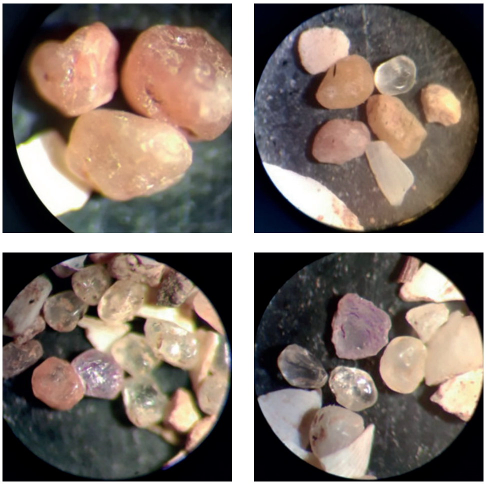

Source: Authors' own studies

Fig. 7. Coloured varieties of quartz

Because quartz (SiO2) is naturally colourless (rock crystal variety),it can take on many other hues, from white, yellow, pink, violet, brown to black (Table 2). The colouring of quartz grains is due to the presence of iron oxides and hydroxides (magnetite, hematite, goethite and limonite). Iron oxides and hydroxides release ferric F3+ into the environment, which first allows surface oxidation (physical alteration) of the grains, and then deep penetration of oxidation leads to the colouring of quartz grains (chemical alteration) (Table 2).

Table 2. The different colours of quartz grains

Some examples of substitution colours		
Color	**Variety**	**Cause**
White	Milky	Diffusion
Yellow to brown	Citrin	Ferric Iron Fe3+
Orange to red		Ferric iron Fe3+
Green	Hematoid	Chlorite
Green		Fuchsite (Mica)
Blue	Prase	Inclusions Ajoite, Azurite...
Purple	Aventurine	Substitution Si^{4+} Fe^{3+}
Pink	Blue	Al^{3+}– P^{3+} Fe^{3+} + or Dumortierite
Grey to brown	Amethyst	Irradiation with Si^{4+} Al^{3+}
Black	Pink, Smoke, Morion	High irradiation

Source: Notari et al. [2001]

The surface oxidation is essentially pedological, indicating a hydrated paleoenvironment. Quartz grains change partly their appearance and colour, their colour is usually observed in the eroded parts of the grains. This phenomenon is linked to hydromorphic degradation of the upper part of the grains.

The chemical alteration of the grains is guided by the crystallographic structures of quartz. By destabilizing the crystal lattice at a very superficial level, dissolution produces lustrous surfaces and geometric shapes in relief and cavities. In unconsolidated, periodically waterlogged environments, weathering of quartz leads to deeper disorganization of the crystal lattice, followed by successive desquamation, resulting in spheroidization of the grains. This chemical alteration also causes Fe3+ to enter the crystal lattice and replaces it with O2-. The result is the colouring of quartz by oxides and hydroxides present in the paleoenvironment (goethite and limonite).

The violet colour is caused by the presence of Fe4+ (by charge transfer O2-Fe4+, Fritsch and Rossman 1988), in substitution of silicon and also interstitially. Natural ionizing radiation produces Fe3+ and Fe4+ coloured centres. Koivula [1989] proposes that the presence of iron is the cause of the formation of polysynthetic macles. This may be due to the amount of iron [Notari and Grobon 2002].

The substitution sites correspond to the tetrahedral sites defined by the Si4+ ion, which is located in the centre of the tetrahedron defined by the first four neighbouring oxygen atoms (O2-).

The violet colouring of quartz grains is caused by the composition of a coloured centre, which in turn is formed by the substitution of Si4+ in the tetrahedra by trivalent iron, with the simultaneous attraction of alkali ions or a proton to make up the charge deficit. X-ray irradiation leads to the formation of the Fe4+ ion, which generates the amethyst colour centre [Zaitov et al. 1974]. Amethyst colouring involves two stages [Balitsky 1999].

During growth, iron +3 is incorporated by the crystal into S sites (Fe3+ substituting for Si4+). The [FeO4]4 – centre, the precursor of the colouring, is then formed. Since it does not interact with light, the crystal is colourless. The second step is to expose the crystal to ionizing radiation of sufficient energy that transforms the [Fe+3O4]4 – centre into a [Fe+4O4]0 centre. As the energy of the y-photons is higher than the binding energy between an electron and the Fe3+ ion, the electron is torn off. It is the [Fe+4O4]0 centre thus formed that interacts with light to produce the violet colour of amethyst. The yellow colour of quartz, which is called citrine, can have several causes, but in general it is due to the absorption of Fe3+ in various forms. In some cases, citrine is coloured by crystalline defects, probably related to Al3+, with a less saturated colour. In citrine from heated amethysts, Fe2+ is found interstitially, or in the form of clusters in which O2-Fe3+ charge transfer takes place. In the case of a citrine centre, the charge deficit is compensated by an alkaline ion and a proton located side by side; the role of charge compensator can be played by an H+ ion.

Citrine colour ranges from yellow to orange and orange-brown. There are many reasons for the differences in colouring. The brown-orange colouring results from the presence of sub-microscopic particles of an unidentified iron oxide, which are captured by the growing faces. Yellow to orange colouring is obtained by heat treatment of amethysts.

The red colour is due to the infiltration of water laden with iron oxides, mainly hematite.

Iron comes mainly from iron oxides and hydroxides, especially magnetite, hematite, goethite and limonite (Table 2). A low concentration of iron, from a few dozen to a few hundred ppm, is sufficient to colour a quartz crystal violet [Filippov et al. 2014].

In our study region, dominated by limestone rocks, the dissolution of diamagnetic minerals, such as calcite, is observed to decrease, with a consequent enrichment in less soluble iron oxides [Eyre and Shaw 1994]. The region's current semi-arid climate favours the formation of hematite, while goethite is formed in a humid climate [Schwertmann and Taylor 1989]. The moderate percentage of SP-sized magnetic grains confirms that this deposit did not experience strong pedogenesis. In general, magnetic susceptibility decreases with depth [Borgne 1955, Singer et al. 1996]. In our case, SM values increase progressively from top to bottom, except for the K and L levels at the base. Could this be due to the migration of fine particles from top to bottom? Both the magnetic and granulometric studies show a stable percentage of fine elements along almost all the stratigraphic section. This suggests a climatic shift from a humid climate at the base (abundant organic matter) to the current semi-arid climate. Indeed, magnetite formation depends on the redox conditions of the environment, which are related to the presence of moisture and organic matter [Borgne 1955, Mullins 1974, Graham and Scollar 1976]. Morphoscopic study demonstrates the presence of a high percentage of transparent flat or strained grains (U).

6. Conclusion, recommendations, and perspectives

This study adopted a comprehensive approach to sedimentological and stratigraphic analysis to unravel the complex history of the study area. Macroscopic field observations facilitated the categorization of the geological section into twelve distinct stratigraphic levels (A to L), providing valuable insights into their composition, texture, and associated features. Granulometric analyses, morphoscopic and exoscopic studies of quartz grains, magnetic methods, and colour analysis further enriched our understanding of sedimentary processes and environmental conditions.

The findings of the granulometric analyses highlighted the alternating richness in coarse fractions and silt at different stratigraphic levels. Ternary diagrams illustrated that the sediments primarily consisted of silts and sands, with specific deposits situated in the silt zone. Morphoscopic and exoscopic examinations of quartz grains provided crucial information about their transport history and alteration processes.

Colour analysis of quartz grains revealed a range of hues, predominantly glassy white to translucent white, along with translucent yellow, orange, and violet shades. A detailed magnetic study confirmed sediment deposition during the late Middle Pleistocene, Late Pleistocene, and Holocene periods under climatic conditions different from the present.

As to recommendations, our study and similar research in the field should consider further exploring the implications of observed granulometric variations in relation to sedimentary processes and environmental conditions, iscussion of the potential significance of identified granulometric fractions in understanding the history of the study area, strengthening of the exoscopy explanation by providing a more comprehensive overview of the scanning electron microscope (SEM) apparatus.

Integration of the magnetic susceptibility data with other sedimentary indicators for a more holistic interpretation.

As to perspectives, we will explore additional analytical techniques such as X-ray diffraction or mineralogical analysis to further characterization sediment components. We will also:

- investigate the application of isotopic analysis for tracing the origin and history of quartz grains,
- extend the discussions to infer broader paleoenvironmental conditions based on sedimentological and granulometric findings, as well as explore the connections between sedimentary characteristics and regional climatic shifts over time,
- collaborate with experts in related fields, such as archaeology or paleobotany, to gain additional insights into the history and evolution of the study area,fostering interdisciplinary discussions for a more comprehensive understanding,
- explore the potential use of advanced techniques, such as high-resolution imaging or elemental mapping, to improve quartz grain characterization, and incorporate statistical analyses to quantify uncertainties and variability in obtained results.

References

Anderson R. 2007. Thematic content analysis (TCA). Descriptive presentation of qualitative data, 3, 1–4.

Balitsky I. 1999. Factorization and high-energy effective action. Physical Review D, 60(1), 014020.

Benmarce K., Hadji R., Zahri F., Khanchoul K., Chouabi A., Zighmi K. 2021. Hydrochemical and geothermometry characterization for a geothermal system in semiarid dry climate: The case study of Hamma spring (Northeast Algeria). Journal of African Earth Sciences, 182, 104285.

Borgne L.E. 1955. Susceptibilité magnétique anormale du sol superficiel. Ann. Geophys., 399–419.

Boulemia S., Hadji R., Hamimed M. 2021. Depositional environment of phosphorites in a semiarid climate region. Case of El Kouif area (Algerian-Tunisian border). Carbonates and Evaporites, 36(3), 1–15.

Cailleux A., Tricart J., Tricart J. 1959. Initiation à l'étude des sables et des galets, 5, Paris, CDU.

Chibani A., Hadji R., Younes H. 2022. A combined field and automatic approach for lithological discrimination in semi-arid regions, the case of geological maps of bir later region and its vicinity, Nementcha mounts, Algeria. Geomatics, Landmanagement and Landscape, 4, 7–26.

Dahoua Lamri R.H., Olena U.S., Viatcheslav Yakovitch S. 2020. Mathematical Approach for Estimating the Stability of Geotextile-Reinforced Embankments During an Earthquake. Mining Science, 25, 207–217.

Dennen W.H. 1966. Stoichiometric substitution in natural quartz. Geochimica et Cosmochimica Acta, 30(12), 1235–1241.

Djerrab A., Aïfa T. 2010a. Stratigraphy and Palaeoenvironment of the Karaïn Cave Infill, Antalya, Turkey. Rock Magnetic Investigations. Studia Geophysica et Geodaetica, 54(1), 49–76.

Djerrab A., Hedley I. 2010. Magnetic mineral study of the Prehistoric site of Caverna delle Fate (Finale, Liguria, Italy). Quaternaire (Paris), 21(2), 165.

Eyre J.K., Shaw J. 1994. Magnetic enhancement of Chinese loess. The role of γFe2O3?. Geophysical Journal International, 117(1), 265–271.

Filippov L., Severov V., Filippova I. 2014. An overview of the beneficiation of iron ores via reverse cationic flotation. Int. J. Miner. Process., 127, 62–69.

Folk R.L., Ward W.C. 1957. Brazos River bar [Texas]. A study in the significance of grain size parameters. Journal of Sedimentary Research, 27(1), 3–26.

Fritsch E., Rossman G.R. 1988. An update on color in gems. Part 2: Colors involving multiple atoms and color centers. Gems and Gemology, 24(1), 3–15.

Graham I.D.G., Scollar I. 1976. Limitations on magnetic prospection in archaeology imposed by soil properties. Archaeo-Physika, 6, 1–124.

Islam A., White R.E., Chen D. 2006. Nitrification activity in acid soils of north-eastern Victoria, Australia, as affected by liming and phosphorus fertilisation. Soil Research, 44(8), 739–744.

Kerbati N.R., Gadri L., Hadji R., Hamad A., Boukelloul M.L. 2020. Graphical and numerical methods for stability analysis in surrounding rock of underground excavations. Example of Boukhadra Iron Mine NE Algeria. Geotechnical and Geological Engineering, 38(3), 2725–2733.

Koivula J.I. 1989. The growth of Brazil twinned synthetic quartz and the potential for synthetic amethyst twinned on the Brazil law. Gems & Gemology, Fall 1989, 159–164.

Laffite J. 1939. Université de Paris. Faculté de droit. La Société nationale des chemins de fer français: thèse pour le doctorat... par Jacques Laffite... Librairie du Recueil Sirey.

Mahleb A., Hadji R., Zahri F., Chibani A., Hamed Y. 2022. Water-Borne Erosion Estimation Using the Revised Universal Soil Loss Equation (RUSLE) Model Over a Semiarid Watershed: Case Study of Meskiana Catchment, Algerian-Tunisian Border. Geotechnical and Geological Engineering, 1–14.

Miskovsky P. 2002. Hypericin – a new antiviral and antitumor photosensitizer: mechanism of action and interaction with biological macromolecules. Current Drug Targets, 3(1), 55–84.

Mullins W.W. 1974. Nonsteady-state particle flow under gravity. An extension of the stochastic theory.

Notari F., Boillat P.Y., Grobon C. 2001. Quartz α-SiO_2: Discrimination des améthystes et des citrines naturelles et synthétiques. Revue de Gemmologie afg, 141(142), 75–80.

Notari F., Grobon C. 2002. Gemmologie du corindon et du spinelle. Corindons et Spinelles, 48–59.

Pye K., Blott S.J. 2004. Particle size analysis of sediments, soils and related particulate materials for forensic purposes using laser granulometry. Forensic Science International, 144(1), 19–27.

Ribault M. 1977. Effet de Haas-van Alphen dans l'ytterbium CFC sous pression. In Annales de Physique, 2, 53–90. EDP Sciences.

Rivière A. 1977. Méthodes granulométriques. Techniques et interprétations.

Schaetzl R.J., Thompson M.L. 2015. Soils: Genesis and geomorphology, 2nd ed. New York, Cambridge University Press.

Schwertmann U.T.R.M., Taylor R.M. 1989. Iron oxides. Minerals in soil environments, 1, 379–438.

Singer M., Ritchot K.F. 1996. The role of working memory capacity and knowledge access in text inference processing. Memory & Cognition, 24(6), 733–743.

Taib H., Benabbas C., Khiari A., Hadji A., Dinar H. 2022. Geomatics-based assessment of the neotectonic landscape evolution along the Tebessa-Morsott-Youkous collapsed basin, Algeria. Geomatics, Landmanagement and Landscape, 3, 131–146.

Taib H., Hadji R., Hamed Y., Bensalem M.S., Amamria S. 2023a. Exploring neotectonic activity in a semiarid basin: a case study of the Ain Zerga watershed. Journal of Umm Al-Qura University for Applied Sciences, 1–14.

Taib H., Hadji R., Hamed Y. 2023b. Erosion patterns, drainage dynamics, and their environmental implications: a case study of the hammamet basin using advanced geospatial and morphometric analysis. Journal of Umm Al-Qura University for Applied Sciences, 1–16.

Taib H., Hadji R., Hamed Y., Gentilucci M., Badri K. 2024. Integrated geospatial analysis for identifying regions of active tectonics in the Saharian Atlas, an review analysis of methodology and calculation fundamentals. Journal of African Earth Sciences, 105188.

Tamani F., Hadji R., Hamad A., Hamed Y. 2019. Integrating remotely sensed and GIS data for the detailed geological mapping in semi-arid regions: case of Youks les Bains Area, Tebessa Province, NE Algeria. Geotechnical and Geological Engineering, 37(4), 2903–2913, 21, 355–365.

Wicander R., Monroe J. 2005. Essentials of Geology. 4th ed., Cengage Learning, Belmont, CA, 510 p.

Zaitov F.A., Shalyapina G.M., Shalyapina L.M., Mukhina O.V. 1974. Effect of an external electric field on the diffusion of impurities in Cdsub (x) Hgsub (1-x) Te. Fizika Tverdogo Tela, 16(4), 1207–1208.

Zeqiri R.R., Riheb H., Karim Z., Younes G., Rania B., Aniss M. 2019. Analysis of safety factor of security plates in the mine 'Trepça' Stantërg. Mining Science, 26(1), 21–30.

Zerzour O., Gadri L., Hadji R., Mebrouk F., Hamed Y. 2020. Semi-variograms and kriging techniques in iron ore reserve categorization: application at Jebel Wenza deposit. Arabian Journal of Geosciences, 13, 1–10.